Journal of Alloys and Compounds 509 (2011) 4987–4991

Contents lists available at ScienceDirect

Journal of Alloys and Compounds

journal homepage: www.elsevier.com/locate/jallcom

Microstructure and tribological properties of NiMo/Mo_2Ni_3Si intermetallic "in-situ" composites

Gui Yongliang*, Song Chunyan, Yang Li, Qin Xiaoling

College of Metallurgy and Energy, Hebei Polytechnic University, 46 Xinhua West Road, Tangshan 063009, PR China

ARTICLE INFO

Article history:
Received 1 May 2009
Received in revised form 25 January 2011
Accepted 27 January 2011
Available online 26 February 2011

Keywords:
Intermetallic
Composite
Microstructure
Wear

ABSTRACT

Wear resistant NiMo/Mo_2Ni_3Si intermetallic "in-situ" composites with a microstructure of ternary metal silicide Mo_2Ni_3Si primary dendritic, the long strip-like NiMo intermetallic phase, and a small amount of Ni/NiMo eutectics structure were designed and fabricated using molybdenum, nickel and silicon elemental powders. Friction and wear properties of NiMo/Mo_2Ni_3Si composites were evaluated under different contact load at room-temperature dry-sliding wear test conditions. Microstructure, worn surface morphologies and subsurface microstructure were characterized by OM, XRD, SEM and EDS. Results indicate that NiMo/Mo_2Ni_3Si composites have low fiction coefficient, excellent wear resistance and sluggish wear-load dependence. The dominant wear mechanisms of NiMo/Mo_2Ni_3Si composites are soft abrasion and slightly superficial oxidative wear.

1. Introduction

The intermetallic composites in the Mo–Si, Nb–Si and W–Si system are of interest as high temperature structure materials because of their high melting point, excellent creep resistance, good oxidation resistance, etc. [1–6]. From the tribological point of view, these silicide-based intermetallic composites have also excellent tribological properties, such as abrasive and adhesive wear resistance as well as low coefficient of friction, due to their intrinsic room- and high-temperature, high hardness and strong atomic bonds [7–9]. While most of early works focused on the binary metal silicides such as $MoSi_2$ and its composites [4–7], some recent studies indicate that ternary metal silicides in the Mo–Ni–Si, W–Ni–Si, Co–Mo–Si, etc. system are a class of promising wear resistance material [10–13].

The ternary transition metal silicide Mo_2Ni_3Si process many attractive properties for application as wear resistant materials. The inherent high hardness and sluggish temperature dependence guarantee Mo_2Ni_3Si outstanding abrasive wear resistance and the strong mixed metallic-covalent atomic bonds provide excellent adhesive wear resistance and low friction coefficient to Mo_2Ni_3Si [14,15]. However, the existence of intrinsic brittleness at ambient temperature and lack of adequate fracture toughness are the main obstacles that prevented the materials from industrial applications as either structural or tribological bulk components. Compared to monolithic metal silicide alloys, multicomponent and multiphase intermetallic composites could have a better combination of toughness and strength [16,17]. Moreover, in an attempt to improve the ductility and fracture toughness of metal silicide alloys, the "in-situ" incorporation of ductile phases has been widely demonstrated being an effective and practical approach among all toughening means [18–20].

In the present work, NiMo/Mo_2Ni_3Si intermetallic "in-situ" composites were designed and produced by arc-melting of elemental starting materials. Microstructure of NiMo/Mo_2Ni_3Si composites was characterized by optical microscopy (OM), scanning electron microscope (SEM), X-ray diffraction (XRD) and energy dispersive spectroscopy (EDS). The dry-sliding wear resistance and friction coefficient at room-temperature of NiMo/Mo_2Ni_3Si composites was evaluated and the corresponding wear mechanisms were discussed.

2. Experimental procedures

Commercially molybdenum, nickel and silicon elemental powders with a particle size from −200 to +400 mesh were selected as the raw materials. The purities of the Mo, Ni and Si starting materials were 99.9, 99.5 and 99.96 wt.%, respectively. The Mo–Ni–Si elemental powder mixture was preheated in an electronic oven at 120 °C for 8–10 h in order to eliminate any absorbed moisture. Nominal chemical composition of the experimental NiMo/Mo_2Ni_3Si intermetallic "in-situ" composite is 36Mo–48Ni–16Si (at.%). More than 20 NiMo/Mo_2Ni_3Si intermetallic "in-situ" composite ingots were prepared by arc-melting process and two or three samples were used for each west test. The ingots were typically remelted 3 times for the purpose of achieving homogeneity prior to metallographic examination and wear test. The melting parameters were taken from previous work and are as follows: electric current about 300 A, voltage 10–12 V, argon protecting and the pressure about 65 kPa.

Metallographic sections of NiMo/Mo_2Ni_3Si intermetallic "in-situ" composites were prepared using standard mechanical polishing and chemical etching pro-

---

* Corresponding author. Tel.: +86 136 5315 7717.
E-mail address: gyl@heut.edu.cn (G. Yongliang).

0925-8388/$ – see front matter © 2011 Elsevier B.V. All rights reserved.
doi:10.1016/j.jallcom.2011.01.179

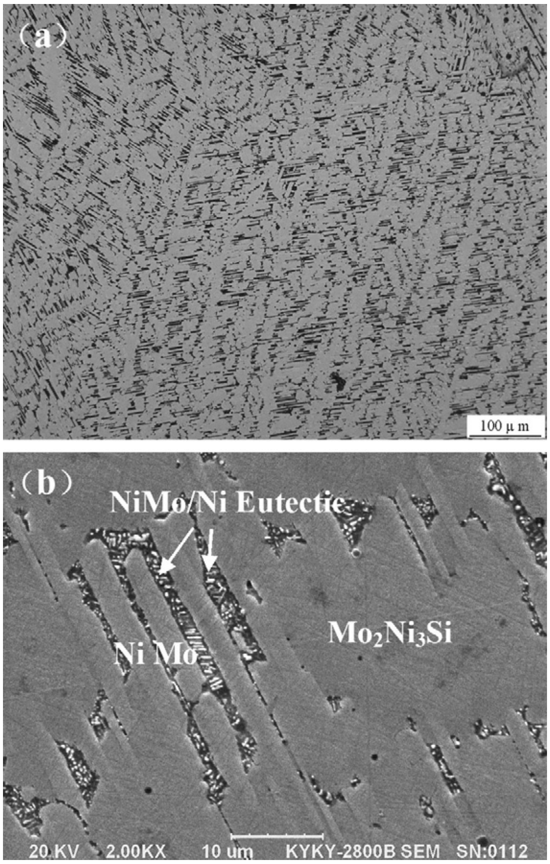

Fig. 1. OM (a) and SEM (b) micrographs showing the microstructure of NiMo/Mo_2Ni_3Si intermetallic "in-situ" composite.

cedures. Microstructure of the experimental composites was characterized using optical microscope (OM) and KYKY-2800 scanning electron microscope (SEM). Phase constituents of the experimental composites were identified by X-ray diffraction (XRD) on Rigaku D/max 2200 pc using Cu K radiation with a scanning rate of 5°/min. Chemical compositions of the phase constituents were analyzed by EDS equipped on KYKY-2800 SEM. Average hardness of the NiMo/Mo_2Ni_3Si intermetallic "in-situ" composites and the hardness of phases were measured using a HXZ-1000 automatic Vickers micro-hardness tester with a test load of 500 g (average hardness of alloy) and 200 g (hardness of phases) respectively and a load-dwell time of 15 s.

Metallic dry-sliding friction and wear tests were performed in a block-on-wheel mode on a MM-200 friction and wear testing machine in air at room temperature. The block-like specimen (10 mm × 10 mm × 10 mm in size) is pressed under a applied test load of 49, 98, 147 and 196 N, respectively, against the outer periphery surface of a hardened 1.0%C–1.5%Cr bearing steel (HRC 63 ± 1) wheel rotating at 400 rpm, resulting in a relative sliding speed of 0.91 m/s and the total sliding distance of 3307 m. The austenitic stainless steel 1Cr18Ni9Ti and hardened 0.45%C steel, the most-widely applied metallic materials, was selected as comparison test materials for all wear tests to rank the wear resistance of the NiMo/Mo_2Ni_3Si intermetallic "in-situ" composites. Wear mass loss of each test was measured using Sartorius BS110 electronic balance with an accuracy of 0.1 mg, and was utilized to rate the wear resistant properties of experimental composites and reference materials. The friction coefficient μ was calculated according to the expression $\mu = T/RP$, where T is the friction torque, R is the wheel radius and P is the contact load on the block-like specimen. The worn surface morphologies, subsurface microstructure and wear debris collected during wear testing process were observed by SEM to analyze wear mechanisms of the NiMo/Mo_2Ni_3Si composites.

3. Results

As shown in Fig. 1a and b, the Mo–Ni–Si alloy ingot has a uniform and dense microstructure consisting of well-developed dendritic primary phase, the long strip-like phase with evident grow-direction, and a small amount of irregular lamellar eutectic structure. X-ray diffraction analysis result indicates that main constitutional phase of the intermetallic composite are the ternary molybdenum nickel silicide Mo_2Ni_3Si, a topologically closed packed (TCP) phase having the hP12 $MgZn_2$ type Laves crystal lattice, and binary intermetallic compound NiMo, as indicated in Fig. 2. Energy dispersive X-ray analysis (EDS) indicates that the well-developed primary dendritic phase with an average chemical composition (at.%) of approximately 31Mo–52Ni–17Si is identified as the Mo_2Ni_3Si ternary metal silicide, the long strip-like phase with an average chemical composition (at.%) of approximately 44Mo–48Ni–8Si is the binary intermetallic compound NiMo, while the irregular lamellar structure is the Ni/NiMo eutectics, the solidification product of the remaining residual liquid.

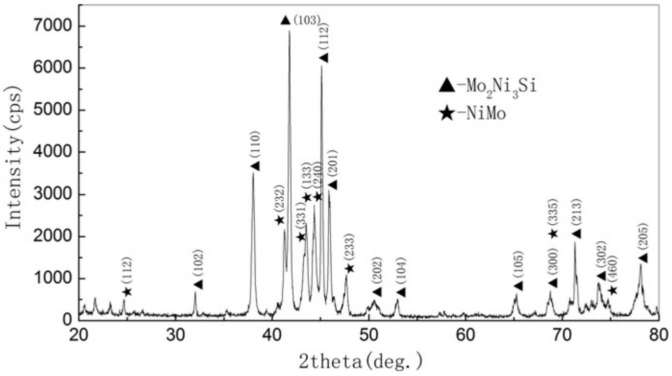

Fig. 2. XRD pattern of the NiMo/Mo_2Ni_3Si intermetallic "in-situ" composite.

The volume fraction of ternary metal silicide Mo_2Ni_3Si for the NiMo/Mo_2Ni_3Si intermetallic "in-situ" composite is approximately 64%. The measured individual hardness of the Mo_2Ni_3Si ternary metal silicide and the NiMo phase are approximately HV1100 and HV930, respectively. Because of the high hardness of NiMo intermetallic phase and the presence of high volume fraction of the hard Mo_2Ni_3Si ternary metal silicide, the NiMo/Mo_2Ni_3Si composite has a high hardness with an average Vickers hardness number of about HV1030. The hardness of reference austenitic stainless steel 1Cr18Ni9Ti and hardened 0.45%C steel is about HV260 and HV640, respectively.

The NiMo/Mo_2Ni_3Si intermetallic "in-situ" composites exhibited outstanding wear resistant properties and low wear-load coefficient under room-temperature dry-sliding wear test conditions coupling with the hardened 1.0%C–1.5%Cr bearing steel mating wheel. As shown in Fig. 3, wear mass loss of the NiMo/Mo_2Ni_3Si intermetallic composite is considerably lower than those of the comparison test materials, the austenitic stainless steel 1Cr18Ni9Ti and hardened 0.45%C steel, under all selected wear

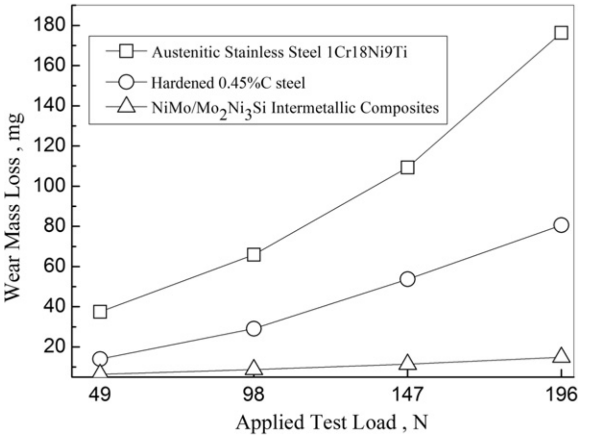

Fig. 3. Wear mass loss of the NiMo/Mo_2Ni_3Si intermetallic "in-situ" composite and the comparison test materials as a function of applied test load under room-temperature dry-sliding wear test conditions.

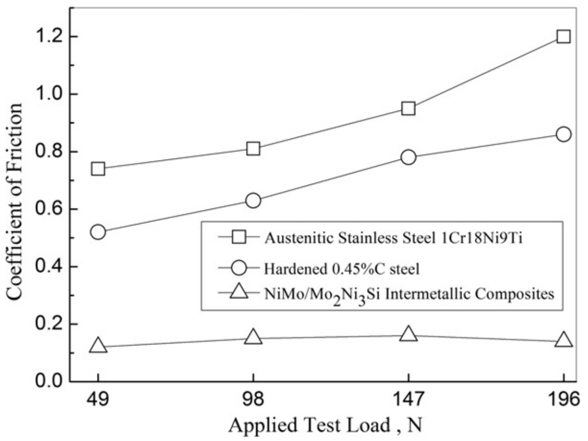

Fig. 4. Friction coefficient of the NiMo/Mo_2Ni_3Si intermetallic "in-situ" composite and comparison materials as a function of contact load under dry sliding wear conditions coupling with hardened 1.0%C–1.5%Cr bearing steel.

test conditions. Wear mass loss of the NiMo/Mo_2Ni_3Si intermetallic composite increase very slowly with increasing test load, whereas those of the austenitic stainless steel 1Cr18Ni9Ti and hardened 0.45%C steel increase obviously with the test load increases.

As shown in Fig. 4, the friction coefficient of the NiMo/Mo_2Ni_3Si composite is lower obviously than that of the austenitic stainless steel 1Cr18Ni9Ti and hardened 0.45%C steel under all contact loads, and is extremely insensitive to the contact load, while that of both comparison materials increases rapidly as the contact load increases from 49 N to 196 N. The low coefficient of friction of is mainly attributed to the high hardness and outstanding adhesive and abrasive wear resistance of the NiMo/Mo_2Ni_3Si intermetallic "in-situ" composite.

As shown in Fig. 5a, the worn surface of the NiMo/Mo_2Ni_3Si intermetallic composite after a dry-sliding wear test cycle of 60 min under the applied test load of 196 N is very smooth and clean except extremely small amount of loosely stuck tiny worn debris particles and some island-like transferred cover layers. Results of EDS analysis indicated that both the transferred cover layers are highly enriched in Fe (approximately 88 at.%Fe), containing little Mo, Ni, Si and O, and hence are predominantly originated from the hardened 1.0%C–1.5%Cr bearing steel counterpart. No any characteristic features of metallic adhesion and abrasive wear such as grooves are observed on the worn surface of NiMo/Mo_2Ni_3Si intermetallic composite (Fig. 5b), whereas noticeable grooves and adhesion and deformation features are visible on the worn surface of the comparison test materials, the austenitic stainless steel 1Cr18Ni9Ti and the hardened 0.45%C steel, as indicated in Fig. 6.

4. Discussion

The excellent wear resistance of the NiMo/Mo_2Ni_3Si intermetallic "in-situ" composite compared to the comparison materials under room-temperature dry-sliding metallic wear test conditions with hardened 1.0%C–1.5%Cr bearing steel as the sliding–mating counterpart (as indicated in Fig. 4) is primarily attributed to the microstructure characteristics and unique chemical and physical properties inherent to the ternary transition metal silicide Mo_2Ni_3Si and binary intermetallic NiMo. Firstly, the ternary metal silicide Mo_2Ni_3Si primary dendrites and binary intermetallic NiMo played the critical role in resisting adhesive wear during metallic sliding wear process and provided the NiMo/Mo_2Ni_3Si intermetallic composite outstanding adhesive wear properties because its unique covalent-dominant strong atomic bonds prevented the intermetallic phase on the very contacting surface from plastic

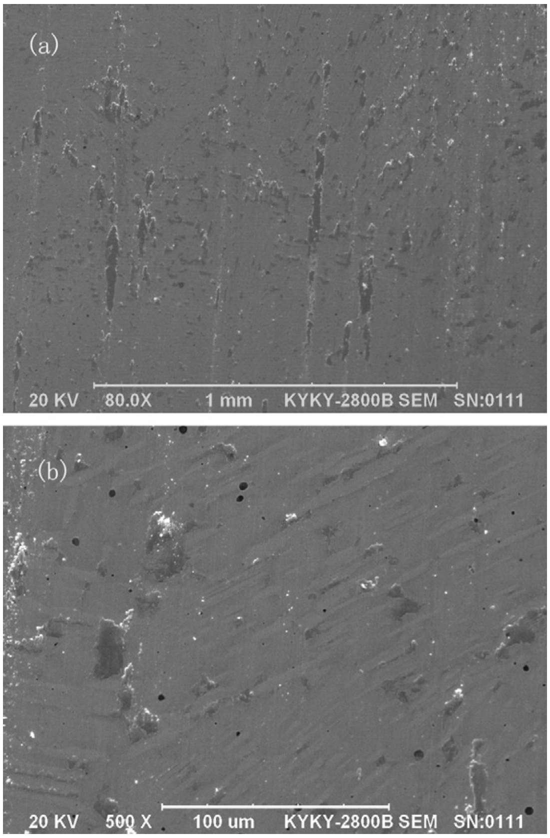

Fig. 5. SEM micrographs showing the worn surface morphologies of the NiMo/Mo_2Ni_3Si intermetallic composite.

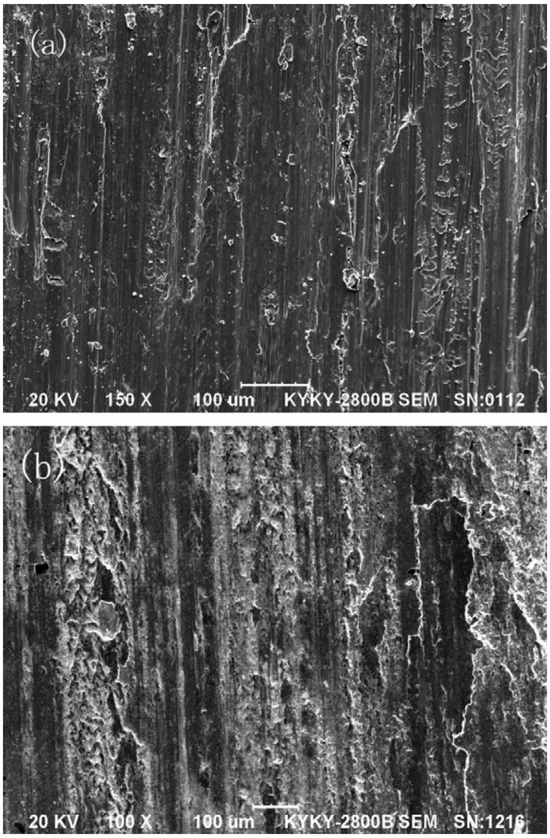

Fig. 6. SEM micrographs showing the worn surface morphologies of the austenitic stainless steel 1Cr18Ni9Ti (a) and hardened 0.45%C steel (b).

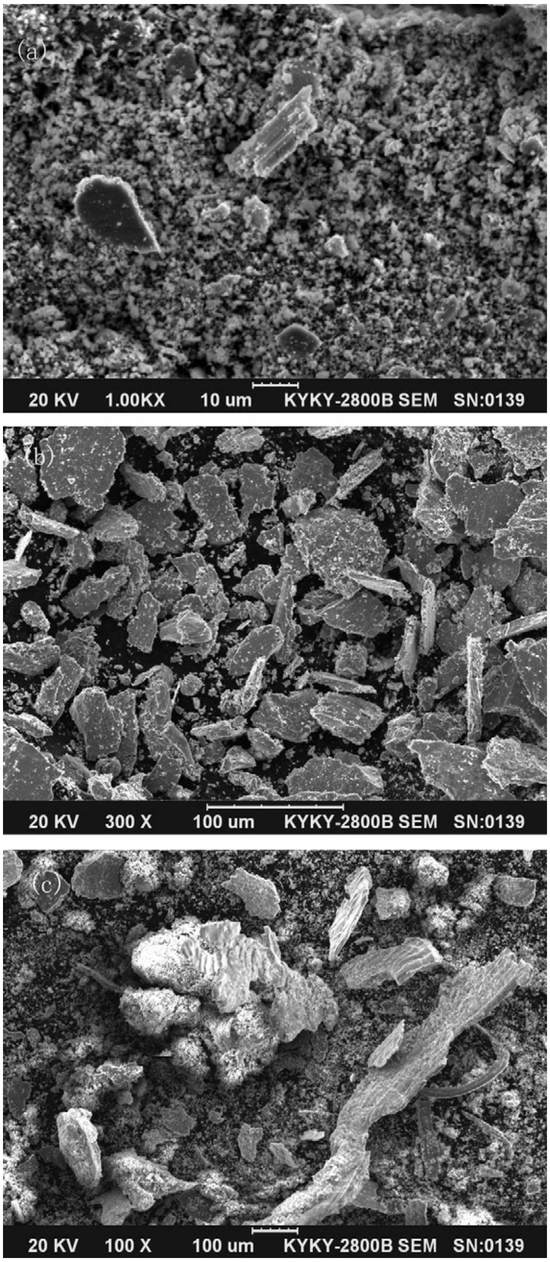

Fig. 7. SEM micrographs of wear debris of the NiMo/Mo_2Ni_3Si intermetallic composite (a), the austenitic stainless steel 1Cr18Ni9Ti (b) and hardened 0.45%C steel (c).

deformation, adhesion and materials-transferring as well as cold-welding to the metallic asperities on the contacting surface of the slide-coupling metallic counterpart. Secondly, both the high hardness of binary intermetallic NiMo and ternary metal silicide Mo_2Ni_3Si and anomalous hardness-temperature dependence of the ternary silicide Mo_2Ni_3Si with the topologically closed-packed (TCP) hP12 $MgZn_2$ type Laves phase crystal structure guarantee the NiMo/Mo_2Ni_3Si intermetallic composite at the very contacting surface with high hardness and hence, excellent resistance to abrasive wear attacks such as micro-cutting and micro-plowing, when dry sliding with surface of the hardened 0.45%C steel coupling wheel under applied pressure. These are evidenced by the very smooth and clean worn surface of the NiMo/Mo_2Ni_3Si intermetallic composite where no any characteristic features of metallic adhesion and abrasive wear are visible, as shown in Fig. 5.

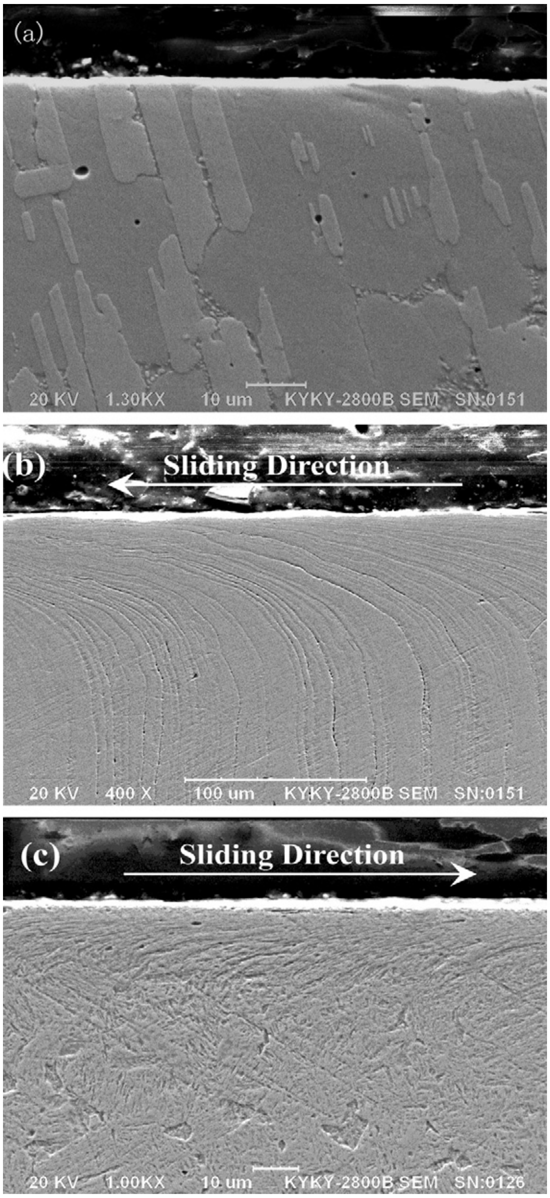

Fig. 8. SEM micrographs showing the worn subsurface microstructure of the NiMo/Mo_2Ni_3Si intermetallic composite (a), the austenitic stainless steel 1Cr18Ni9Ti (b) and hardened 0.45%C steel (c).

SEM observations indicate that all wear debris particles of NiMo/Mo_2Ni_3Si intermetallic composite are in tiny powders, flake-like and loosely agglomerated powder clusters, while the wear debris of the austenitic stainless steel 1Cr18Ni9Ti and the hardened 0.45%C steel is in very large and thick flakes, as shown in Fig. 7. Further EDS analysis indicates that the tiny powders and loosely agglomerated powder clusters are highly enriched in Fe and O with small amount of Mo, Ni and Si, and are actually the complex oxides. This result indicated that the superficial oxidation of experimental materials and counterpart occurred during dry-sliding wear process, due to the friction-induced temperature rise on the very contact sliding surface. The chemical composition of flake-like debris examined by EDS analysis is similar to transferred cover layers (Fig. 5a) which is highly enriched in Fe (approximately 88 at.%Fe) with negligible amount of Mo, Ni, Si and O. Therefore, the tiny powders and loosely agglomerated powder clusters are identified as the iron oxides particles which are primarily originated from the contacting surface of mating hardened

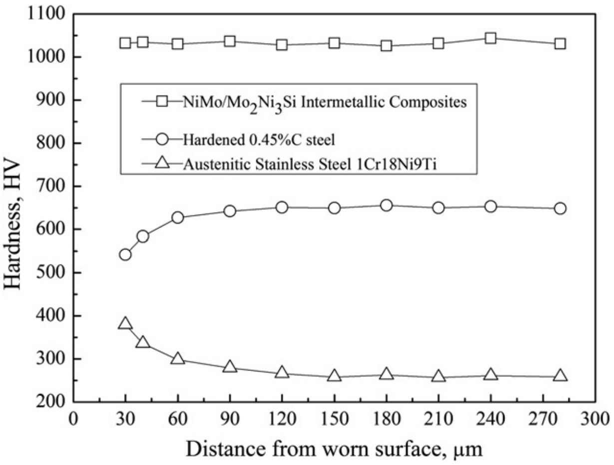

Fig. 9. Subsurface hardness profiles of the NiMo/Mo_2Ni_3Si intermetallic composite and the comparison materials on longitudinal section along wear sliding direction perpendicular to worn surface.

1.0%C–1.5%Cr bearing steel counterpart, and the flake-like debris is most likely the rolling-consolidated "sheet-like" product of tiny powders agglomerates entrapped between the rolling wheel and the NiMo/Mo_2Ni_3Si intermetallic composite block-like specimen.

To investigate carefully the wear mechanisms, worn subsurface microstructures beneath the worn surface of the test materials on longitudinal section along the wear sliding direction and perpendicular to worn surface were studied. No evidence of local plastic deformation, brittle fracture and selective wear to NiMo and Mo_2Ni_3Si phases in NiMo/Mo_2Ni_3Si intermetallic composite were observed, while serious subsurface plastic deformation occurred for the austenitic stainless steel 1Cr18Ni9Ti and the hardened 0.45%C steel, as shown in Fig. 8. All the aforementioned wear test phenomena indicate that the dominating wear mechanisms of NiMo/Mo_2Ni_3Si intermetallic composite under room-temperature dry-sliding wear test condition are soft abrasion and slightly superficial oxidative wear.

As indicated in Figs. 8 and 9, the NiMo/Mo_2Ni_3Si intermetallic "in-situ" composites keep high strength and hardness all along even at a large load owing to its inherent high hardness and anomalous hardness-temperature relation, and hence have a quite low wear mass loss under all wear test conditions, while the hardened 0.45%C steel is significantly softened due to the friction heating during wear process, and then more severely deformed and the wear mass loss increased drastically with the increasing test load (Fig. 4). The most severe plastic deformation occurred on the subsurface of austenitic stainless steel 1Cr18Ni9Ti owing to the lowest one hardness in three test materials, as shown in Fig. 8. However, the work-hardening effect is obviously detected in the plastic deformation zone of the subsurface of austenitic stainless steel 1Cr18Ni9Ti, and softening phenomenon caused by friction heating is not evidenced because of the more outstanding high-temperature properties. Although that, the wear mass loss is higher and the wear-load dependence is more obviously than NiMo/Mo_2Ni_3Si intermetallic composites since the hardness is still lower.

In summary, the NiMo/Mo_2Ni_3Si intermetallic "in-situ" composites can neither be plastically deformed, microcut or plowed, nor microfractured or cracked under the dry-sliding interaction of the metallic friction counterparts, therefore, the NiMo/Mo_2Ni_3Si composites can only be very slowly worn off by the mechanism of soft-rubbing of the hardened 1.0%C–1.5%Cr bearing steel counterpart and slightly oxidative worn on high temperature contact surface induced by the friction heat.

5. Conclusions

Wear resistant NiMo/Mo_2Ni_3Si intermetallic "in-situ" composites were fabricated successfully with Mo–Ni–Si powder blends as the starting materials. Microstructure of the NiMo/Mo_2Ni_3Si composites consists of Mo_2Ni_3Si primary dendrites, binary intermetallic phase NiMo and small amount of Ni/NiMo eutectics structure. The NiMo/Mo_2Ni_3Si composites exhibited high hardness and outstanding tribological properties under room-temperature dry-sliding wear test conditions which were attributed to the covalent-dominant strong atomic bonds and excellent combination of strength and ductility and toughness.

References

[1] K. Sadananda, C.R. Feng, R. Mitra, S.C. Deevi, Mater. Sci. Eng. A 261 (1999) 223–238.
[2] F. Wang, A.D. Shan, X.P. Dong, J.S. Wu, J. Alloys Compd. 459 (2008) 362–368.
[3] N. Sekido, Y. Kimura, S. Miura, F.G. Wei, Y. Mishima, J. Alloys Compd. 425 (2006) 223–229.
[4] W.Y. Kim, H. Tanaka, S. Hanada, Intermetallics 10 (2002) 625–634.
[5] P.V. Krakhmalev, J. Bergström, Wear 260 (2006) 450–457.
[6] I.J. Shon, D.H. Rho, H.C. Kim, Z.A. Munir, J. Alloys Compd. 322 (2001) 120–126.
[7] J.W. Newkirk, J.A. Hawk, Wear 251 (2001) 1361–1371.
[8] H.A. Zhang, X.P. Hu, J.H. Yan, Wear 260 (2006) 903–908.
[9] T.S.R.Ch. Murthy, B. Basu, A. Srivastava, J. Eur. Ceram. Soc. 26 (2006) 1293–1300.
[10] X.D. Lu, H.M. Wang, Appl. Surf. Sci. 245 (2005) 346–352.
[11] H.M. Wang, D.Y. Luan, L.X. Cai, Metall. Mater. Trans. A 34 (2003) 2005–2015.
[12] Y. Liu, H.M. Wang, Scripta Mater. 52 (2005) 1235–1240.
[13] Y.L. Fang, H.M. Wang, J. Alloys Compd. 433 (2007) 114–119.
[14] X.D. Lu, H.M. Wang, Surf. Coat. Technol. 200 (2005) 2380–2385.
[15] X.D. Lu, H.M. Wang, Acta Mater. 52 (2004) 5419–5426.
[16] A. Misra, R. Gibala, Intermetallics 8 (2000) 1025–1034.
[17] K. Nihara, Y. Suzuki, Mater. Sci. Eng. A 216 (1999) 6–15.
[18] J.H. Schneibel, M.J. Kramer, Ö. Ünal, Intermetallics 9 (2001) 25–31.
[19] R. Mitra, A.K. Srivastava, N.E. Prasad, Intermetallics 14 (2006) 1461–1471.
[20] H. Choe, D. Chen, J.H. Schneibel, Intermetallics 9 (2001) 319–329.